Original Article

Inhibition of NLRP3 attenuates sodium dextran sulfate-induced inflammatory bowel disease through gut microbiota regulation

*Shi-Le Wang [a], Man-Man Zhang [a], Han Zhou [a], Guo-Qiang Su [c], Yi Ding [d], Guang-Hui Xu [e], Xu Wang [b], Cheng-Fu Li [g], Wei-Feng Huang [b,f,**], Li-Tao Yi [a,h,i,*]*

[a] *Department of Chemical and Pharmaceutical Engineering, Huaqiao University, Xiamen, Fujian, China*
[b] *Department of Gastroenterology, The First Affiliated Hospital of Xiamen University, School of Medicine, Xiamen University, Xiamen, Fujian, China*
[c] *Department of Colorectal Cancer Surgery, The First Affiliated Hospital of Xiamen University, School of Medicine, Xiamen University, Xiamen, Fujian, China*
[d] *Department of Pathology, The First Affiliated Hospital of Xiamen University, School of Medicine, Xiamen University, Xiamen, Fujian, China*
[e] *Xiamen Medicine Research Institute, Xiamen, Fujian, China*
[f] *The School of Clinical Medicine, Fujian Medical University, Fuzhou, Fujian, China*
[g] *Xiamen Hospital of Traditional Chinese Medicine, Xiamen, Fujian, China*
[h] *Institute of Pharmaceutical Engineering, Huaqiao University, Xiamen, Fujian, China*
[i] *Fujian Provincial Key Laboratory of Biochemical Technology, Huaqiao University, Xiamen, Fujian, China*

ARTICLE INFO

ABSTRACT

Background: Inflammatory bowel disease (IBD) is a chronic, life-threatening inflammatory disease of gastrointestinal tissue characterized by inflammation of the gut. Recent studies have shown that gut microbiota is involved in the pathophysiology of IBD. However, it is unknown whether direct inhibition of NLR family pyrin domain containing 3 (NLRP3) inflammasome regulates IBD and alters gut microbiota.

Methods: Here, the NLRP3 expression was evaluated in the colon of IBD subjects. Then, we investigated the effects of NLRP3 inhibition by MCC950 on the gut microbiota and IBD-like symptoms induced by dextran sulfate sodium (DSS).

Results: Firstly, NLRP3 and IL-1β levels were increased in patients with IBD as compared with healthy individuals. Then, the animal experiment showed that NLRP3 inhibition by MCC950 significantly attenuated IBD-like symptoms such as diarrhea and colonic inflammation in DSS-induced mice. In addition, NLRP3 inhibition inhibited NLRP3/ASC/caspase-

 * Corresponding author. Department of Chemical and Pharmaceutical Engineering, Huaqiao University, 668, Jimei Avenue, Xiamen 361021, Fujian, China.
 ** Corresponding author. Department of Gastroenterology, The First Affiliated Hospital of Xiamen University, School of Medicine, Xiamen University, 422, Siming South Rd., Xiamen 361003, Fujian, China.
   E-mail addresses: hwf0625@xmu.edu.cn (W.-F. Huang), litaoyi@hqu.edu.cn (L.-T. Yi).
   Peer review under responsibility of Chang Gung University.

1/IL-1β signaling pathway in the colon, which was over-activated by DSS. Furthermore, MCC950 increased the abundance of phylum Firmicutes, decreased the abundance of phylum Bacteroidetes, and increased the Firmicutes/Bacteroidetes ratio, indicating that the inhibition of NLRP3 inflammasome could regulate the abundance of intestinal flora. According to correlation analysis, NLRP3 might produce its functional role in the regulation of oxidation indicators by changing the gut microbiota composition, especially the phylum Bacteroidota, genus *Lactobacillus* and species *Lactobacillus reuteri*.

Conclusions: This study suggests that NLRP3 inflammasome inhibition attenuates IBD-like symptoms by regulating gut microbiota, and provides a basis for the clinical application of NLRP3 as a target for the treatment of IBD.

At a glance commentary

Scientific background on the subject

NLRP3 inflammasome, an important component of innate immunity, is involved in the development and progression of several inflammatory diseases. Previous studies have shown that NLRP3 inflammasomes are dysregulated in IBD models, and over-activated NLRP3 inflammasomes enhance colonic mucosal injury and exacerbate DSS-induced colitis in mice.

What this study adds to the field

This study indicates that NLRP3 signaling is over-activated in IBD patients. The inhibition of NLRP3 reverses the IBD-like symptoms in DSS-induced mice via the regulation on gut microbiota. This study also provides a basis for the clinical application of NLRP3 as a target for the treatment of IBD.

Introduction

Inflammatory bowel disease (IBD) is a chronic, life-threatening inflammatory disease of gastrointestinal tissue characterized by gut inflammation. IBD is mediated by self-acquired T lymphocytes and is a chronic disease that recurs over time [1,2]. In recent years, the incidence of IBD has been increasing year by year, with a high incidence in European and American countries and a sharp increase in developing countries including South America, Asia, Africa, and Eastern Europe [3,4]. Clinically, the patient presents with abdominal pain, diarrhea, and persistent purulent bloody stool [5]. Generally, inflammatory enteritis is divided into Crohn's Disease and Ulcerative Colitis according to different onset locations and characteristics.

It has been widely accepted that genetic, gut microbial, environmental, and inflammatory factors are involved in the pathogenesis of IBD [6]. Inflammatory factors have been considered crucial pathogenesis that is likely to be explored for a potential treatment for IBD [7]. Inflammasomes have been considered vital players in innate immunity. The inflammasomes are cytosolic multiprotein oligomers that modulate inflammation in response to the stimulus. The most

characterized is NLR family pyrin domain containing 3 (NLRP3) inflammasome, which is highly relevant to inflammation reaction and plays an important role in the human body and animals [8]. It can be easily found in immune cells like macrophages. Activated NLRP3 will promote many downstream effector proteins like cytokine [9]. Cytokines like interleukin-1 beta (IL-1β) can mediate inflammation reactions, mainly by increasing the number of macrophages to the targeting location or tissue [10—13]. With a huge number of macrophage functioning, the targeting tissue or location is likely to suffer severe inflammation. If the targeting location is set to the intestine or its related area, IBD might be caused.

An abnormal gut microbial community has also been considered a vital factor that causes IBD [14]. There has been evidence showing that patients with IBD have abnormal gut microbial flora in clinical and experimental research [15]. Generally, normal intestinal microbial balance will benefit the organisms or tissues [16]. However, the disturbance of the gut microbial community might lead to detrimental microbe overgrowth, which may stimulate intestinal tissue and cause an inflammation reaction [17]. Inflammation reaction, in return, might cause a more serious unbalance of the gut microbial community. Chronic inflammation in the intestine might then lead to severe IBD [18,19].

In this study, we found that NLRP3 and IL-1β were typically increased in patients with IBD as compared with healthy individuals. In this respect, we tried to investigate whether NLRP3 inhibition could alleviate IBD symptoms induced by dextran sulfate sodium (DSS) in mice. In order to further elucidate the potential mechanism of NLRP3 inhibition against IBD, the NLRP3 signaling in the colon and the microbiota composition in the gut were measured.

Material and method

Human colon samples

The normal intestinal tissues were obtained from the patients with polyps for endoscopic resection. The pathological intestinal tissues were obtained from IBD patients for endoscopic mucosal biopsies. There were 6 normal participants and 6 IBD participants in the present study. The average ages were 43.5 ± 3.2, 45.3 ± 2.9 years. The gender ratio of participants is 1:1. The human body study was approved by the ethics review committee of the First Affiliated Hospital of Xiamen University (No.2022−038) and carried out in accordance with the Helsinki Declaration of the World Medical Association. We have

obtained informed and confirmed written consent from the normal participants and patients.

Animals

Eight weeks old and body-weighted 24 ± 2 g ICR mice were obtained from Shanghai Slac Animal Center (Shanghai, China). The mice have been raised with standard laboratory purified water and standard food, and the temperature was set to 22 ± 2 °C, and the humidity was set to 55 ± 5%. They were adapted to the environment for 1 week before the beginning of the experiment. All procedures are carried out in accordance with the guidelines of the Laboratory Animal Management Regulations and the Laboratory Animal Management System of Huaqiao University and have been approved by the Laboratory Animal Management Committee of Huaqiao University (A2021002).

Reagents

MCC950 (M6164) was purchased by AbMole BioScience (Houston, USA). DSS (D122354, MW 40000) was purchased from Aladdin Reagent Co., Ltd (Shanghai, China). Anti-β-actin (A3854) was purchased from Sigma (St. Louis, USA). Anti-NLRP3 (ab214185), Anti-IL-1β (ab9722), anti-interleukin-6 (IL-6, ab9324), and Anti-Iba1 (ab5076) were purchased from Abcam (Cambridge, USA). Anti-cleaved caspase-1 (89332) was purchased from Cell Signaling Technology (Beverly, USA). Anti-ASC (SC-514414) was purchased from Santa Cruz Biotechnology (Dallas, USA). Anti-tumor necrosis factor-alpha (TNF-α, AF8208) was purchased from Beyotime Biotechnology (Shanghai, China). Malondialdehyde (MDA, A003-1-2), catalase (CAT, A007-1-1), and superoxide dismutase (SOD, A001-3-2) assay kits were purchased from Nanjing Jiancheng Bioengineering (Nanjing, China).

Drug treatment

All the mice were randomly divided into four groups (n = 12): normal-vehicle group; normal-MCC950 group; DSS-vehicle group; DSS-MCC950 group. MCC950 is dissolved into 5mg/10 ml with PBS (equivalent to a dose of 5 mg/kg). DSS is dissolved into 0.25mg/10 ml with PBS. Normal-MCC950 and DSS-MCC950 group mice were weighed and injected intraperitoneally with MCC950 at an injection volume of 10 mL/kg throughout the experiment. Normal-vehicle and DSS-vehicle were injected intraperitoneally with PBS at the same injection volume of 10mL/10 kg for 14 days as well. DSS solution (2.5%) was given to mice in DSS-vehicle and DSS-MCC950 group for 8 days (from day 7 to day 14) to induce mice IBD model.

Assessment of colon inflammation severity

The disease activity index has been widely used in the DSS-induced model. Here, we used it to assess the severity of rectal inflammation severity. The disease activity index mainly includes a score of rectal bleeding and stool consistency [20]. The colons were obtained immediately after the mice were sacrificed, and the length of the colons was measured. All parameters were scored from day 7 to day 14. The details of the disease activity index scoring standard have been shown in Table 1.

Colonic histologic scoring

The score of colonic histology was blindly assessed according to the following parameters (Part I) inflammatory infiltration (0 = none, 1 = inflammatory cells above muscularis serosa only, 2 = inflammatory cells in submucosa, 3 = inflammatory cells in muscularis serosa to muscularis mucosa, or 4 = extensive inflammation in mucosa and epithelial layer) (Part II) crypt damage (0 = none, 1 = <30%, 2= <60%, 3 = only epithelial surface intact, or 4 = entire crypt and epithelia lost) (Part III) goblet cell depletion (0 = none or 1 = present), and (iv) crypt abscess (0 = none or 1 = present). Subsequently, Parts I-III were multiplied by a degree factor of 1 = focal, 2 = patchy, or 3 = diffused.

Analysis for MDA, CAT and SOD

The blood was collected and clotted at room temperature for 10 min, followed by centrifugation at 3000g for 20 min. The supernatant was collected and stored in a −80 °C refrigerator for assays according to the instructions of the manufacturers.

Western blotting

RIPA tissue cell lysate was used to extract the proteins in colons. After adding RIPA lysate and PMSF, the samples were homogenized and then centrifuged, and the supernatant was collected. The BCA method has been used to quantify protein in the supernatant, followed by adding 5 × loading buffer and then boiling in 90 °C water for 5 min. Each sample has been separated by SDS-PAGE and then transferred to the PVDF membrane. The membrane was blocked Quick blocking solution for 15 min. Primary antibodies (1:1000) were added and then incubated overnight on the shaker at 4 °C. TBST-tween 20 was used to wash the membrane 3 times for 5 min each time on the next day. Then the secondary antibody (1:5000) was added and incubated on the shaker at room temperature for 1 h. The membrane was rewashed 3 times, and then an ECL developer was added for gray-level analysis in the Chemiluminescence Imager System.

Immunofluorescence

The human tissues were fixed in 4% paraformaldehyde followed by dehydration with alcohol. Then the dehydrated tissues were embedded with paraffin. 5 μm thickness of the paraffin sections was cut for further staining. In detail, xylene and alcohol were first used to remove the paraffin from the

Table 1 Score of disease activity index.	
Stool Consistency	Rectal Bleeding
1 = normal	1 = normal color
2 = loose stools	2 = brown color
3 = diarrhea stools	3 = reddish color
4 = Liquid stools	4 = bloody color

sections. Then the sections were immersed in antigenic repair solution and blocking solution, respectively. NLRP3 or IL-1β antibody (1:150) was added to incubate sections overnight. After incubating with the secondary antibody for 3 h, the sections were incubated with DAPI for 5 min. The sections were finally observed under a laser scanning confocal microscope (Leica TCS SP8) and photographed.

Mice were injected with 4% chloral hydrate to anesthesia. 0.1 mol/L PBS was used to infuse through the left ventricular. After the liver turned white, 4% paraformaldehyde was perfused for fixation. The colons from the mice were obtained and then embedded with OCT frozen agent, followed by 15 μm thickness of the frozen section. Immunostaining fixative solution was used for fixation and then washed by TBST-triton 3 times for 5 min each time. Antigenic repair solution was then spread on the section for 5 min, and washed by TBST-triton 3 times again. The section was then blocked by immunofluorescence blocking solution for 1 h, and then the primary antibody was added and incubated at 4 °C overnight. On the next day, the section was washed with TBST-triton 3 times again, and then the secondary antibody was incubated at room temperature for 3 h. After incubation, the section was again washed with TBST-triton for 3 times, followed by incubating DAPI at room temperature for 5 min. The colon was observed under a laser scanning confocal microscope (Leica TCS SP8) and photographed.

During the immunofluorescence detection, identical settings in a confocal microscope were used to acquire images for all samples. The images were photographed, selected, and analyzed from either humans or mice by a blinded observer to the treatment. To determine NLRP3/ASC/IL-1β levels, 20× plus zoom in single-plane images were collected. Areas of NLRP3/ASC/IL-1β surface were automatically calculated.

Gut microbiota analysis

The total DNA of the intestinal flora of each group of mouse colon contents was extracted according to the instructions of the DNA extraction kit. The DNA was quantified by gel electrophoresis to detect the quality of the total DNA. PCR amplification was then performed on the variable regions of the 16 S rRNA gene V3−V4, and three replicates were performed for each sample. The recovered PCR products were purified and detected according to the instructions of the DNA Gel Recovery Kit, and the recovered products were quantified by fluorescence. The sequences were sequenced on the Illumina Miseq PE300 platform to obtain the original sequencing sequences. Based on the 97% similarity, the processed sequences were grouped into multiple chimera-free operational taxonomic units using Majorbio Cloud (https://cloud.majorbio.com/). The taxonomic information was used for statistical analysis of community structure at different taxonomic levels.

Statistical analysis

All data were performed and presented as mean ± SEM. The basic criterion for sample size estimate is that the SEM should be less than 10% of the Mean. One-way ANOVA was used for comparisons between IBD and normal individuals. Two-way ANOVA followed by Tukey's test was used for comparisons

between every two groups. Statistical analysis was performed with GraphPad Prism v7.0. A value of $p < 0.05$ was considered as a significance.

Results

NLRP3 and IL-1β expression is increased in the colon of IBD subjects

To investigate whether NLRP3 and IL-1β expression is changed in IBD subjects, we conducted an immunofluorescence analysis of colon samples collected from IBD patients and age-matched individuals without IBD. We found a significant increase in NLRP3 (Fig. 1A and B) and IL-1β (Fig. 1C and D) expression in colon samples obtained from IBD subjects compared to control subjects.

NLRP3 inhibition alleviate the symptoms in DSS-induced IBD mice

In order to assess the protective effect of NLRP3 inhibition on IBD, DSS was used to induce IBD-like symptoms in mice (Fig. 2A). The stool consistency and rectal bleeding were measured in the present study. The image of the anus in Fig. 2B reflected that NLRP3 inhibition alleviated the severe diarrhea levels in response to DSS consumption. As shown in Fig. 2C, DSS significantly increased the score of the disease activity index as compared with the normal mice. On the contrary, NLRP3 inhibition significantly improved DSS-induced IBD symptoms, as the score of the disease activity index was significantly reduced by MCC950. Subsequently, we measured the length of colon after animal sacrifice. As shown in Fig. 2D and E, DSS shortened the length of colon in mice, while NLRP3 inhibition tended to attenuate the change. Finally, histopathological examination revealed that DSS caused goblet cell reduction, crypt destruction, and epithelial barrier disruption, indicating colonic inflammation and tissue damage in mice. NLRP3 inhibition could alleviate these histopathological changes and scores of colons in DSS-induced mice (Fig. 2F and G).

The effects of NLRP3 inhibition on the levels of the oxidation indicators SOD, CAT, and MDA levels in the serum

As shown in Fig. 3, DSS significantly decreased the levels of CAT activity and tended to decrease SOD activity [$p = 0.061$] in the serum compared with the normal-vehicle group. The inhibition of NLRP3 with MCC950 remarkably reversed the reduction of CAT and SOD activities in the serum, indicating that NLRP3 inhibition promoted the antioxidant capacity in mice.

On the other hand, neither DSS nor MCC950 altered MDA levels in the serum.

NLRP3 inhibition inhibited colon NLRP3/ASC/IL-1β signaling induced by DSS

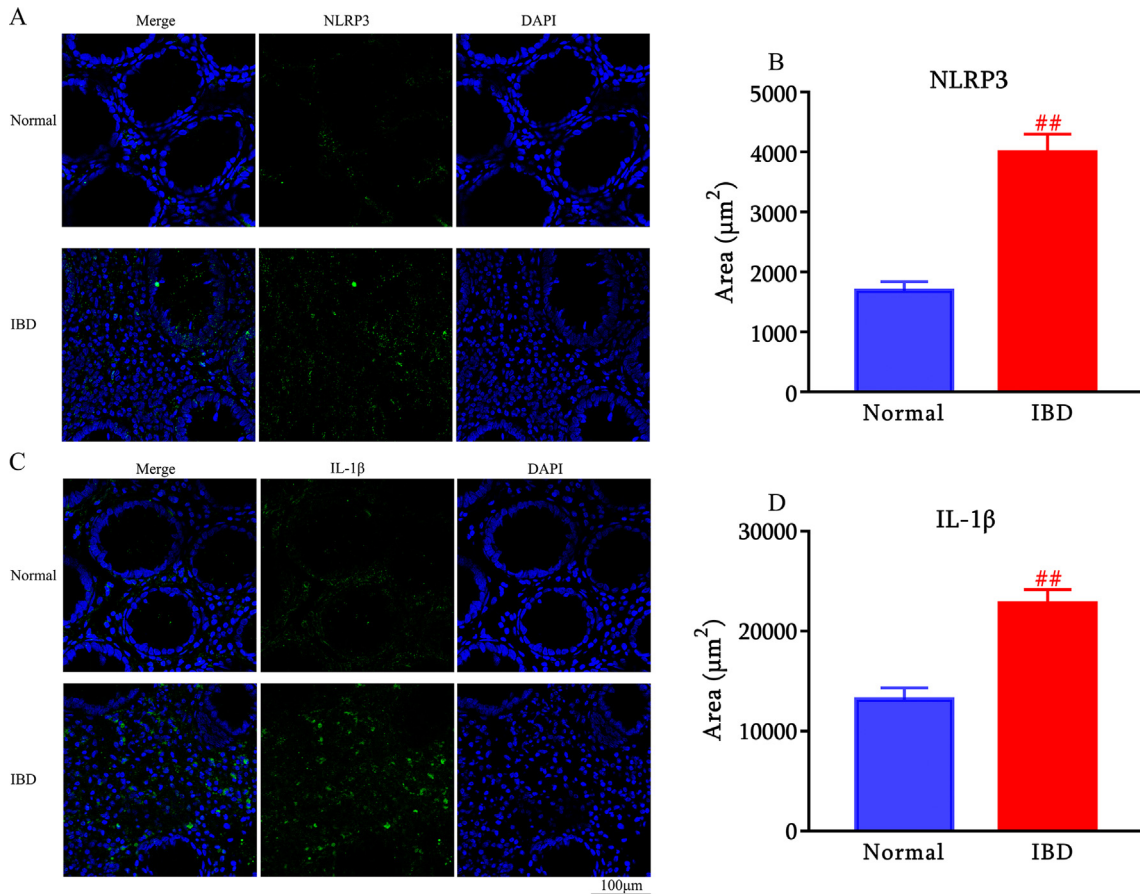To check the inhibitory effect of MCC950 in DSS-induced IBD mice, the core components of NLRP3/ASC/IL-1β signaling

Fig. 1 NLRP3 and IL-1β are over-expressed in IBD patients (n = 6). Representative images of NLRP3 immunostaining in distal colon of normal individuals and IBD patients. Scale bar: 100 μm (A). Quantification of NLRP3 (B). Representative images of IL-1β immunostaining in the colon of normal individuals and IBD patients. Scale bar: 100 μm (C). Quantification of IL-1β (D). $^{\#\#}p < 0.01$ compared with normal individuals.

pathway were detected by both Western blot (Fig. 4) and immunofluorescence (Fig. 5).

According to the results from the Western blot, DSS significantly induced the elevation of NLRP3 in the colon, while MCC950 treatment significantly reduced the NLRP3 levels. Consistently, ASC, the adaptor of NLRP3 inflammasome, which was enhanced by DSS, was remarkably inhibited by MCC950. Besides, IL-1β, one of the effectors of NLRP3, was highly inhibited by MCC950 in DSS-induced colon.

Similarly, the immunofluorescence showed that MCC950 produced an inhibitory trend of NLRP3/ASC/IL-1β in the colon.

NLRP3 inhibition reshaped the gut microbiota in DSS-induced IBD mice

According to the gut microbiota analysis, a total of 559 OTU in Normal-vehicle group, 628 OTU in DSS-vehicle group, 498 OUT in Normal-MCC950 group, and 581 OTU in DSS-MCC950 group were detected according to Venn diagram (Fig. 6A). Then we used beta diversity to examine the consistency of the microbial community of all samples. Based on PCA analysis on OTU level, DSS group presented a distinct clustering of OUT among the four groups (Fig. 6B). On the contrary, there was no difference between DSS-MCC950 group and Normal-vehicle group, indicating that the gut microbiota was restored in the presence of MCC950 intervention in DSS mice.

As shown in Fig. 6C-F, DSS decreased the relative abundance of Phylum Firmicutes but increased the relative abundance of Phylum Bacteroidota, while MCC950 reversed the changes. The top 11 relative abundance of Phylum level among the four groups at the phylum level was displayed in a heatmap. As shown in Fig. 6G-I, DSS decreased the relative abundance of Genus Lactobacillus but increased the relative abundance of Genus Bacteroides, Enterorhabdus, Alloprevotella and Lachnospiraceae. In contrast, MCC950 reversed the abnormalities in fecal. The top 20 relative abundance of Genus level among the four groups at the phylum level was displayed in a heatmap.

Next, we used LEfSe algorithm to identify the characteristic microbiota in each group (Fig. 7). By setting an LDA threshold
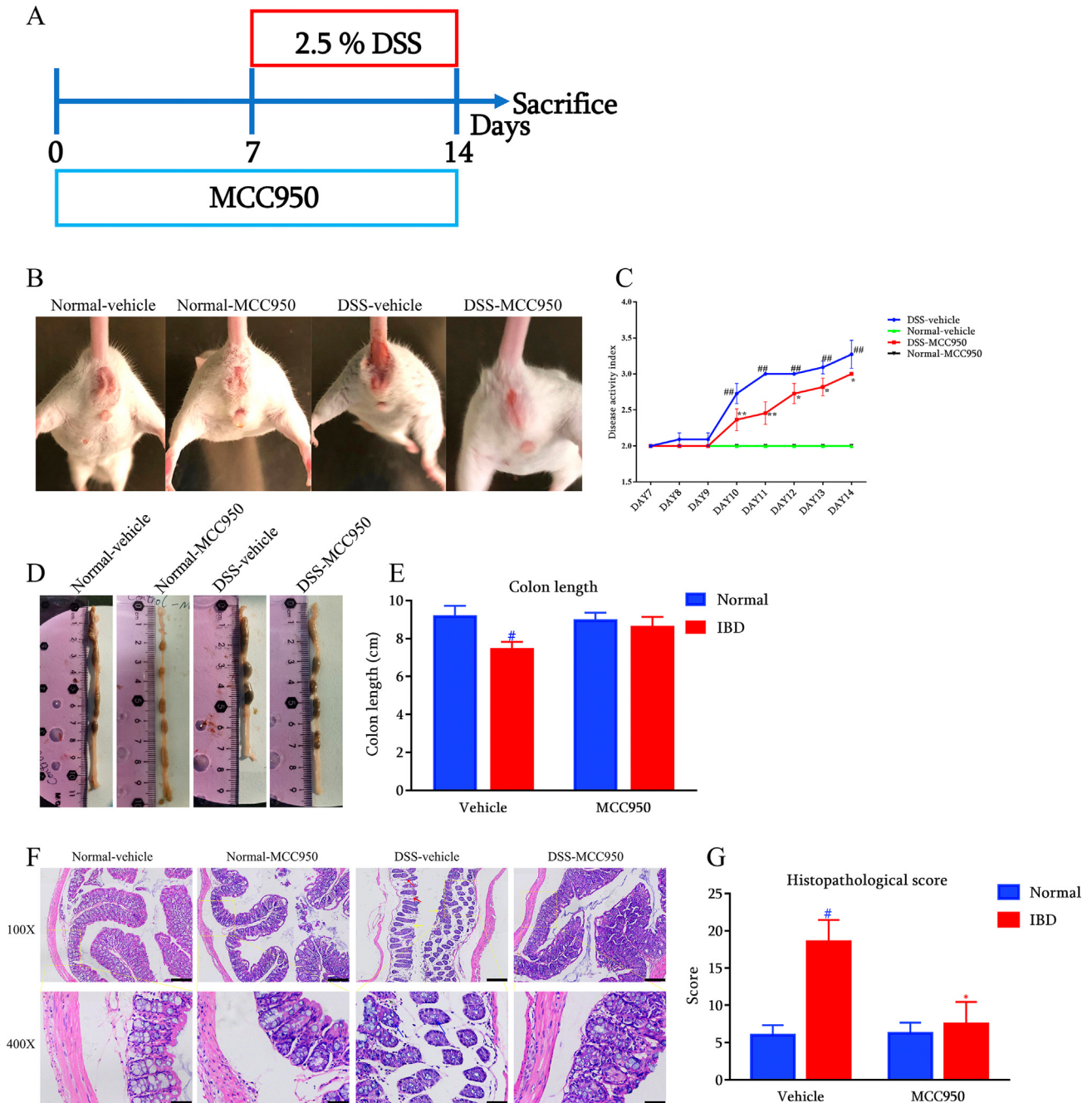
Fig. 2 NLRP3 inhibition with MCC950 attenuated IBD-like symptoms in DSS-induced mice (n = 11) (A) Diagram for the experimental protocol (B) Representative diarrhea (C) Disease activity index during DSS consumption (D) Representative colon length and (E) statistical results (F) H&E staining and (G) histopathological scores of distal colons (Red arrow indicates crypt destruction, yellow arrow indicates epithelial barrier disruption, and blue arrow indicates goblet cell reduction. Scale bar = 200 μm above, Scale bar = 50 μm below). #$p < 0.05$ and ##$p < 0.01$ compared with Normal-vehicle group; *$p < 0.05$ and **$p < 0.01$ compared with the DSS-vehicle group.

greater than 4 and $p < 0.05$, the analysis identified 29 prokaryotic clades. In the DSS group, the taxa with significantly higher abundance belonged to Phylum Bacteroidota and Genus Bacteroides. MCC950 group showed a high abundance of Phylum Firmicutes and Family Lactobacillaceae. DSS-MCC950 group showed a high abundance of Phylum Proteobacteria and Genus *Clostridia*.

The correlation analysis between gut microbiota and inflammatory activity or oxidation indicators

A Spearman correlation analysis was performed to elucidate further the relationship between the altered gut microbiota and inflammatory activity or oxidation indicators (Fig. 8). The relative abundance of phylum Bacteroidota showed a
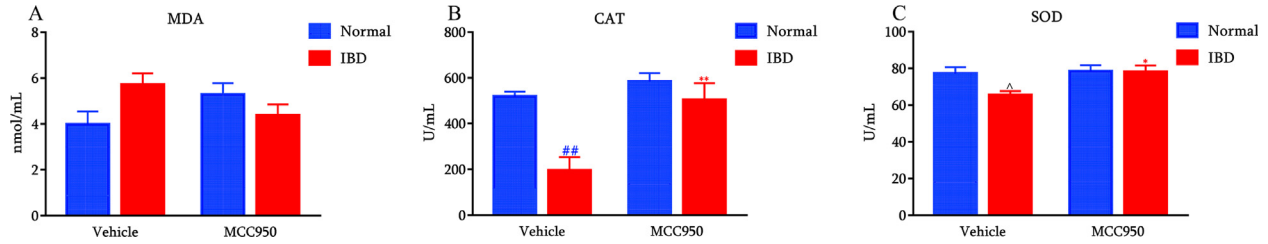
Fig. 3 Effects of NLRP3 inhibition on oxidation indicators such as MDA (A), CAT (B) and SOD (C) levels in serum (n = 6). $^{##}p < 0.01$ and $\hat{}p = 0.061$ compared with Normal-vehicle group; $*p < 0.05$ compared with the DSS-vehicle group.

significant positive correlation with NLRP3 and IL-1β (Fig. 8A), the abundance of genus *Lactobacillus* showed a significant negative correlation with NLRP3, caspase-1 and IL-1β (Fig. 8B), and the abundance of species *Lactobacillus reuteri* showed significant negative correlation with NLRP3 (Fig. 8C). These observations mean that the inhibition of NLRP3 enhanced the relative abundance of phylum Bacteroidota, but decreased the relative abundance of genus *Lactobacillus* and species *L. reuteri*, which might be involved in the regulation of inflammation.

In addition, the relative abundance of phylum Firmicutes showed a significant positive correlation with CAT and SOD (Fig. 8D), the abundance of genus *Lactobacillus* showed a significant positive correlation with CAT and SOD, but a negative

correlation with MDA (Fig. 8E), and the abundance of species *Lactobacillus intestinalis* showed a significant positive correlation with SOD (Fig. 8C). These results demonstrated that NLRP3 might produce its functional role in regulating oxidation indicators by changing the gut microbiota composition, especially the phylum Firmicutes, genus *Lactobacillus* and species *L. intestinalis*.

Discussion

IBD is a group of intestinal diseases characterized by the appearance of complex inflammatory responses in the small and large intestines. The role of NLRP3 inflammasome in IBD
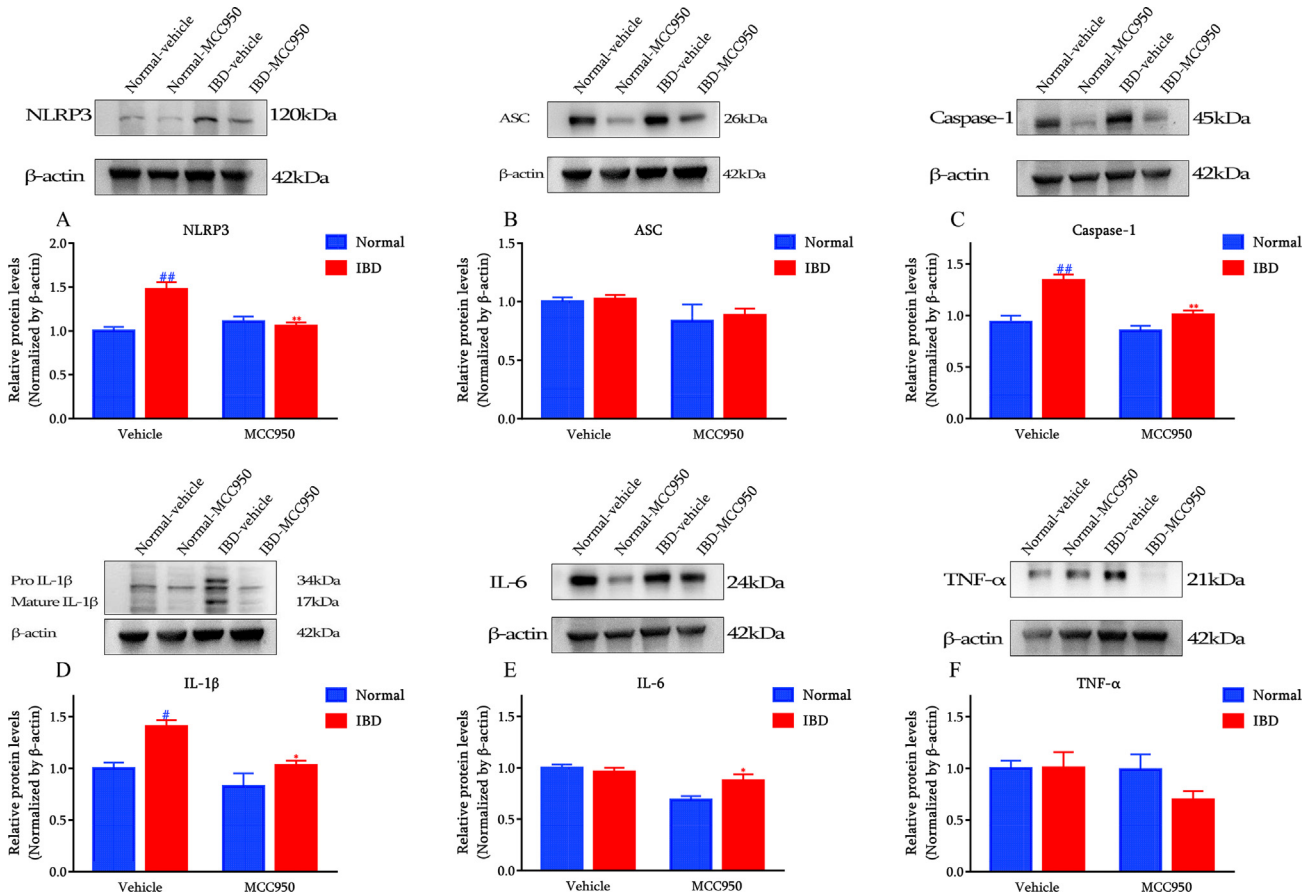

Fig. 4 MCC950 inhibited DSS-induced NLRP3 pathway and decreased pro-inflammatory cytokines in distal colon (n = 5) (A) NLRP3 (B) ASC (C) Caspase-1 (D) IL-1β (E) IL-6 (F) TNF-α. $^{#}p < 0.05$ and $^{##}p < 0.01$ compared with Normal-vehicle group; $*p < 0.05$ and $**p < 0.01$ compared with the DSS-vehicle group.
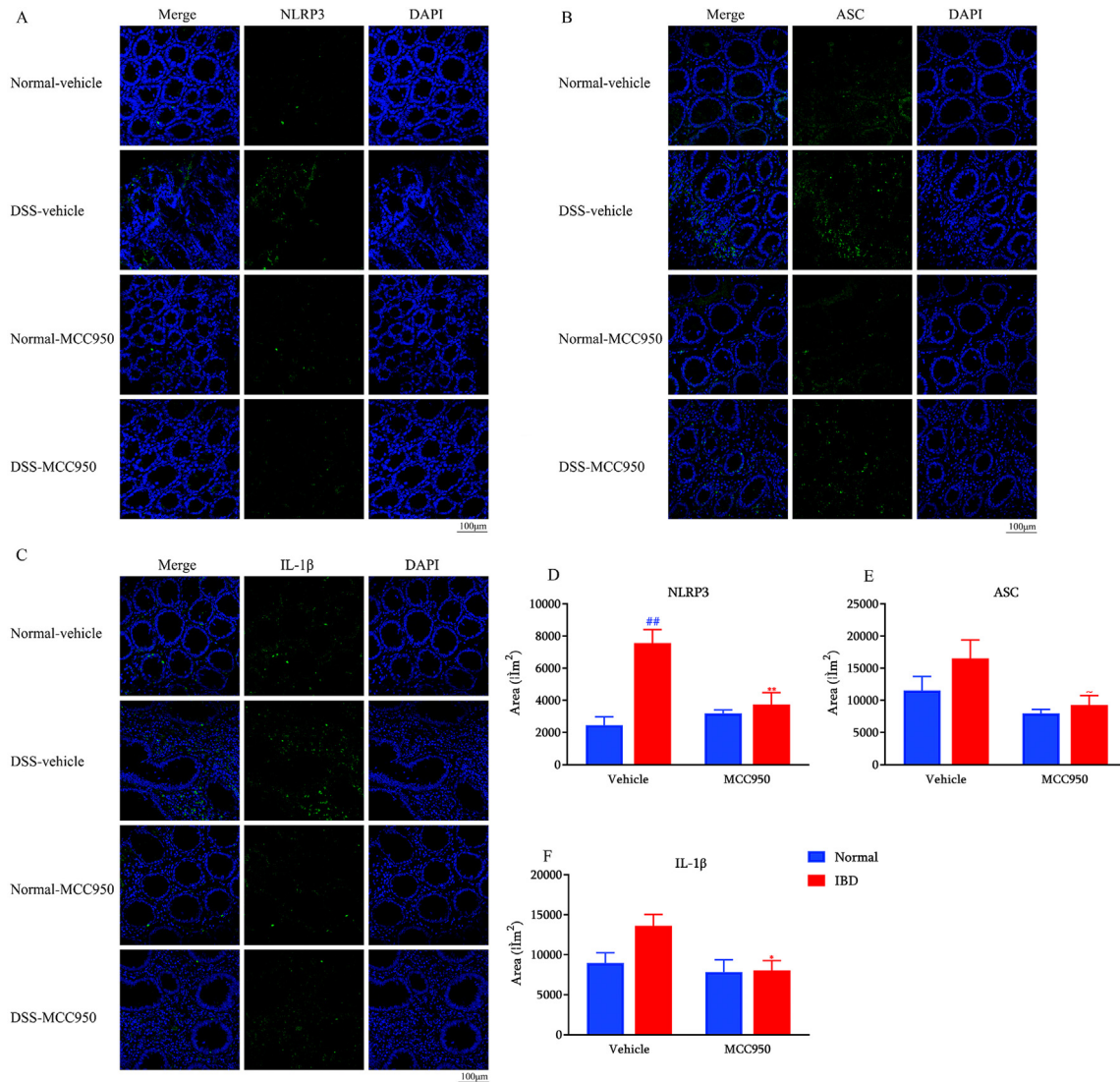
Fig. 5 MCC950 inhibited DSS-induced NLRP3/ASC/IL-1β signaling pathway in distal colon (n = 4). Representative immunostaining images of (A) NLRP3 (B) ASC, and (C) IL-1β. $^{##}p < 0.01$ compared with Normal-vehicle group; $*p < 0.05$, $**p < 0.01$ and $\tilde{}p = 0.083$ compared with the DSS-vehicle group.

is still controversial. Most studies show that activated NLRP3 is involved in the pathogenesis of DSS-induced colitis in mice [21]. However, it has also been found that lack of any component of NLRP3 inflammasome results in mice highly susceptible to DSS-induced colitis. These defective inflammasomes disrupt the loss of intestinal epithelial cell integrity, leading to systemic dispersion of intestinal bacteria and increased production of inflammatory factors [22]. This study collected colonic tissues from IBD patients and healthy subjects. By using immunofluorescence, we found a significant increase in NLRP3 expression in IBD patients as compared with healthy normal. Consistently, a significant increase in IL-1β, a cytokine regulated by NLRP3, was also observed in IBD patients, suggesting that the NLRP3 inflammasome-mediated cytokine pathway is involved in the pathogenesis of IBD. The results of these clinical observations were consistent with those reported by Lazaridis et al. [23].

The DSS-induced IBD model has been widely used to investigate intestinal inflammation, and DSS-induced animals exhibit features such as diarrhea, colonic bleeding, and even death [24]. Histopathological analysis indicates that DSS-induced animals show extensive epithelial cell damage in colorectal tissues with marked macrophage and neutrophil infiltration, tissue edema, and ulcer formation; these features are similar to the pathological features of clinical IBD patients [25,26]. In this study, the results indicated that the animals developed diarrhea and the anus began to become red and swollen after oral consumption of 2.5% DSS for 7 days. Abdominal dissection revealed significant shortening of the colon and marked inflammatory features of the colonic tissue. Direct inhibition of NLRP3 inflammasome activity using MCC950 attenuated DSS-induced IBD symptoms, including improvement in fecal morphology, anal erythema, colonic length, and morphology of colonic tissues. This is partly
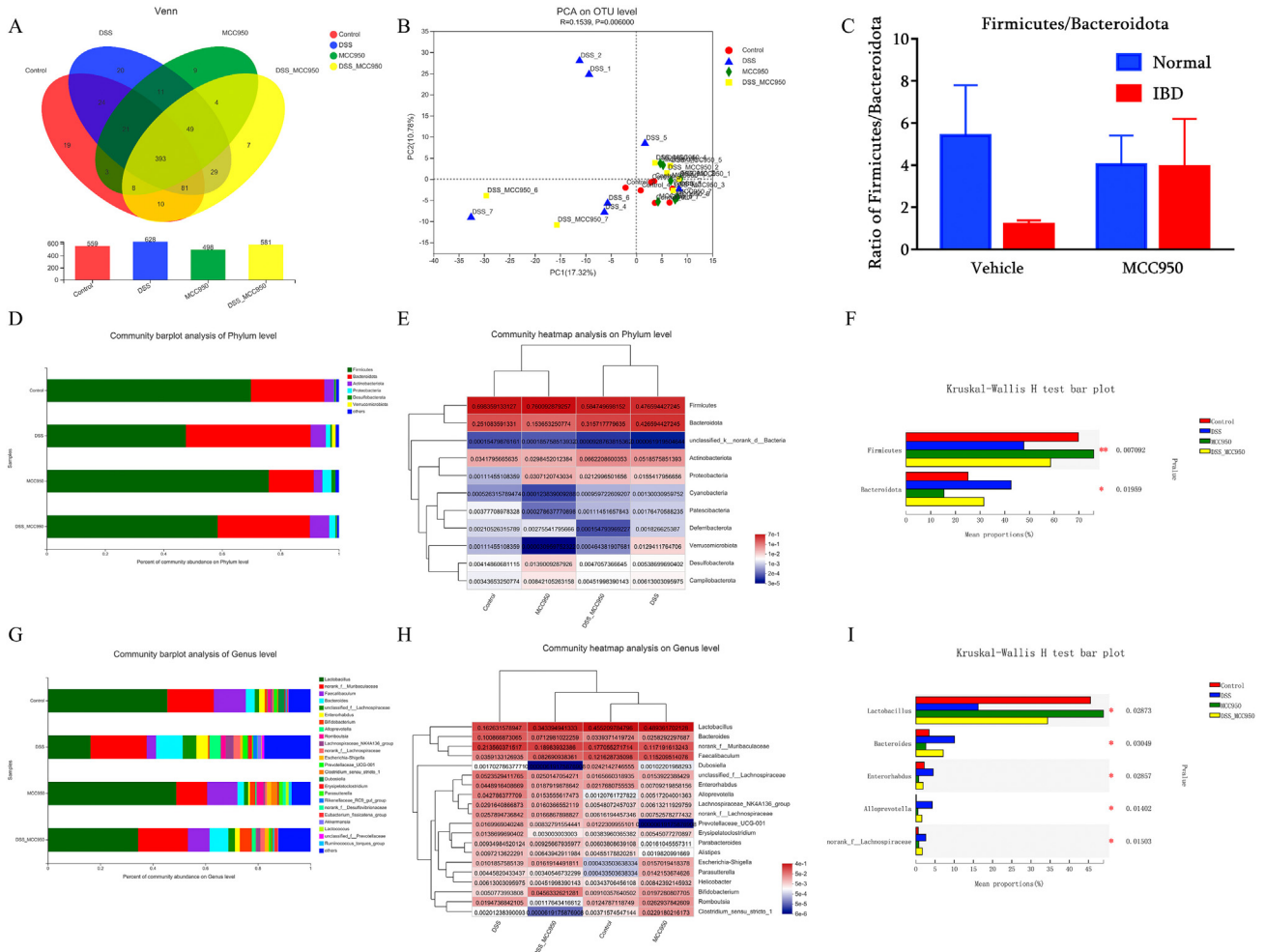
Fig. 6 NLRP3 inhibition with MCC950 modulates gut microbiota diversity and composition in DSS-induced IBD mice (n = 7) (A) Venn diagrams showing the number of differential gut microbiota and their shared gut microbiota at the OTU level (B) Beta diversity of PCA (C) The relative abundance ratio of Firmicutes/Bacteroidota among the groups (D) Relative abundance (E) heatmap, and (F) predominant of taxa at the phylum level (G) Relative abundance (H) heatmap, and (I) predominant of taxa at the genus level. *p < 0.05 and *p < 0.01.

consistent with a previous study showing that treatment with MCC950 reduced intestinal inflammation in Nod2$^{-/-}$ mice, a gene knockout animal exhibiting increased expression of NLRP3 inflammasome and IL-1β [27].

The role of immune factors in the pathogenesis of IBD has been widely recognized. Abnormal immune responses are considered an important part of the pathogenesis of IBD. It is generally accepted that IBD occurs when environmental factors act on genetically susceptible individuals and subsequently activate macrophages and lymphocytes, releasing a series of cytokines and inflammatory mediators that can further regulate and mediate the immune response, leading to humoral and cellular immune responses that persist and expand step by step, resulting in intestinal damage and a range of clinical manifestations [28,29]. NLRP3 inflammasome, an important component of innate immunity, is involved in the development and progression of several inflammatory diseases. Previous studies have shown that NLRP3 inflammasomes are dysregulated in IBD models, and

over-activated NLRP3 inflammasomes enhance colonic mucosal injury and exacerbate DSS-induced colitis in mice [30]. Therefore, targeting and regulating the activation of NLRP3 inflammasome will provide new approaches and strategies for the treatment of IBD. We found that the expression of NLRP3 inflammasome, ASC, caspase-1, and IL-1β were significantly increased in the colonic tissues of IBD mice, indicating the over-activation of the NLRP3 signaling pathway. In addition, the expression of other pro-inflammatory cytokines, IL-6 and TNF-α were also significantly increased, indicating a severe inflammatory response in the colon. In contrast, the activation of NLRP3 inflammasome signaling in the colon was inhibited by MCC950 treatment, and the pro-inflammatory cytokines IL-1β, IL-6, and TNF-α were also significantly reduced. Combined with the findings that MCC950 improved IBD symptoms, the results suggest that reducing cytokine expression through direct inhibition of NLRP3 inflammasome could effectively alleviate intestinal inflammation.
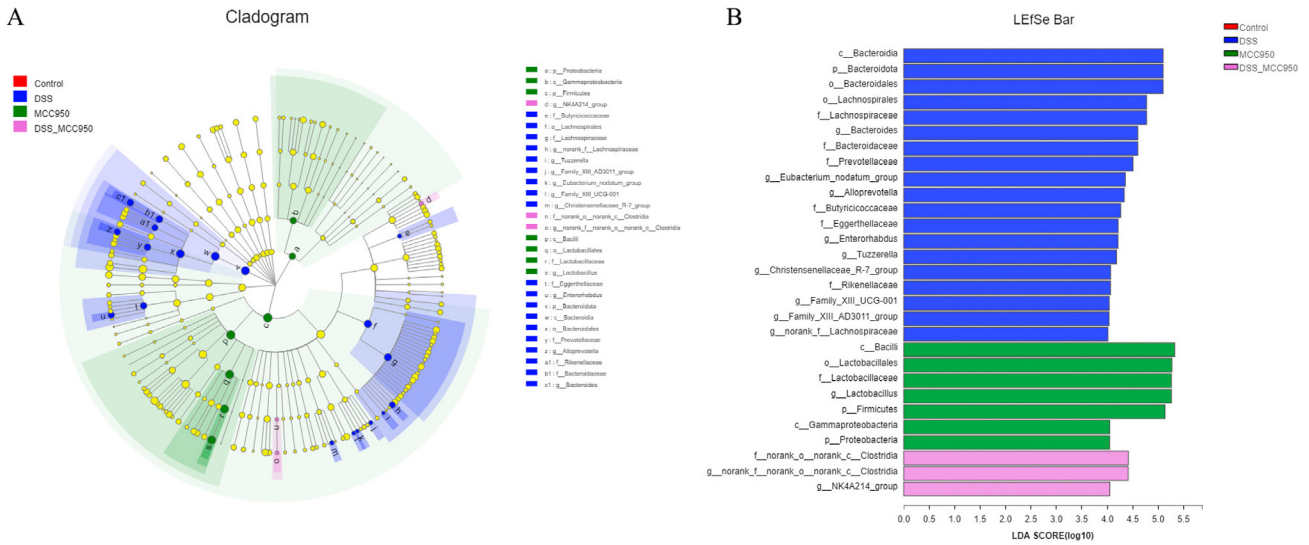
Fig. 7 The LEfSe analysis of microbial abundance in DSS-induced IBD mice (n = 7) (A) The cladogram generated by LEfSe analysis (B) The taxa with a significant difference were obtained by LEfSe analysis (LDA threshold = 4, p < 0.05).
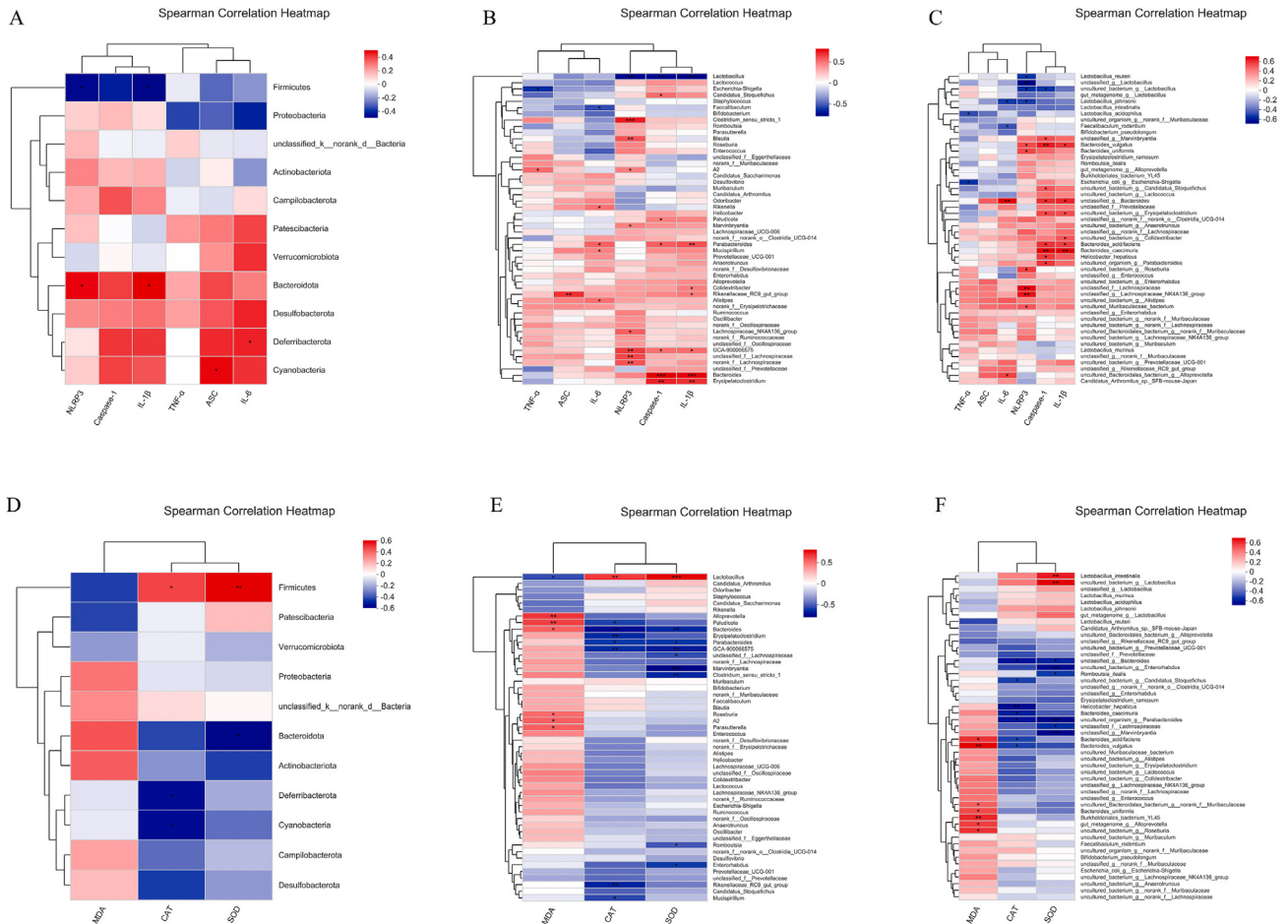

Fig. 8 Heatmap summarizes Spearman's correlation (n = 5). Between serum oxidation indicators and gut microbiota at (A) phylum (B) genus, and (C) species level. Between colon inflammation and gut microbiota at (D), phylum(E) genus, and (F) species level. *p < 0.05 and **p < 0.01.

NLRP3 can exacerbate the inflammatory response by causing cells to secrete large amounts of IL-1β inflammatory factors through the caspase-1/IL-1β pathway; it can also mediate pyroptosis through activation of Gasdermin D (GSDMD), inducing cell membrane perforation, causing massive distention and necrosis of tissue cells, allowing the efflux of cell contents, and further amplifying the inflammatory response [31]. For example, GSDMD pores are large enough to allow the transport of mature IL-1β [32]. Evidence has shown that patients or animals with IBD are accompanied by increased expression of epithelial-derived GSDMD, indicating that GSDMD is involved in the pathogenesis of IBD [33−35]. When the agonist NEK7 of NLRP3 is knocked out, the activation of caspase-1 and the release of IL-1 β are restricted [36]. In DSS-induced IBD mice, the knockout of NEK7 was associated with decreased levels of NLRP3, caspase-1, and GSDMD [37]. This observation suggests that pyroptosis, which is regulated by NLRP3/GSDMD may be a new treatment strategy for IBD. Meanwhile, in a previous clinical study, quantitative analysis of mucosal biopsy samples from IBD patients revealed that the inhibition of pyroptosis in intestinal epithelial cells is a potential mechanism for mesalazine treatment of IBD [38]. In this respect, we can speculate that NLRP3 blockade might protect DSS-induced IBD against intestinal barrier disruption also by inhibiting NLRP3/caspase-1/GSDMD-mediated pyroptosis in the colon. Of course, considering that the relationship between NLRP3/GSDMD-mediated pyroptosis and intestinal inflammation is complicated, further studies involving pyroptosis assessment are required to clearly elucidate the role of pyroptosis in MCC950-treated IBD.

The intestinal microbiota has an important impact on the development and disease progression of IBD. Certain intestinal bacteria can disrupt the intestinal mucosa and invade the mucosal epithelium, induce monocytes and macrophages to produce large amounts of pro-inflammatory cytokines, and mediate severe inflammatory responses [30]. Therefore, regulation of intestinal microflora is one of the important ways to treat IBD. While numerous previous studies have shown that probiotic administration is beneficial in preventing or treating IBD [12,39], the present study is the first to examine the effects of direct inhibition of NLRP3 inflammasome on the gut microbiota DSS-induced IBD. The results showed that DSS-induced IBD was accompanied by dysbiosis of the intestinal flora, consistent with previous studies on IBD involving dysbiosis of the intestinal flora [40]. In addition, we found that direct inhibition of NLRP3 inflammasome could modulate the microbial community structure in IBD. Generally, Firmicutes and Bacteroidetes, the two most crucial bacterial phylum in the gut, dominate the intestinal microecosystem, and we found that Firmicutes and Bacteroidetes accounted for more than 90% of the total colonies in both normal and IBD animals. Generally, phylum Firmicutes consists of Gram-positive bacteria such as *Bacillus*, *Clostridium*, *Enterococcus,* and *Lactobacillus*, while the phylum Bacteroidetes consists of Gram-negative bacteria such as *Bacteroides*, *Parabacteroides,* and *Prevotella* [41]. In this study, the abundance of phylum Firmicutes was significantly lower in IBD mice, while the abundance of phylum Bacteroidetes was significantly increased. The results were consistent with the clinical observations, which found a significant decrease in the abundance of phylum Firmicutes [42] and a significant increase in the abundance of phylum Bacteroidetes [43] in the intestine of IBD patients compared to healthy individuals. More importantly, the abundance of phylum Firmicutes was closely related to the severity of IBD disease, with the more severe the IBD symptoms, the lower the abundance of phylum Firmicutes [44]. Interestingly, the Firmicutes and Bacteroidetes (F/B) ratio was also closely correlated with the onset and progression of IBD. After mucosal biopsy and gene extraction of IBD patients, the F/B ratio of IBD patients was found to be significantly lower than that of normal healthy individuals [45,46]. In parallel to this clinical investigation, this study also found that the intestinal F/B ratio of DSS-induced IBD mice was lower than that of normal mice. In contrast, MCC950 administration increased the abundance of phylum Firmicutes, decreased the abundance of phylum Bacteroidetes, and increased the F/B ratio, indicating that the inhibition of NLRP3 inflammasome could regulate the abundance of intestinal flora, maintain intestinal homeostasis, and move the intestinal microbiota in IBD in a direction favorable to the organism. Indeed, in other animal models, it has been observed that the inhibition of NLRP3 inflammasome reduced the abundance of phylum Bacteroidetes, increases the F/B ratio, and improves intestinal homeostasis in autoimmune encephalomyelitis [47].

In conclusion, this study provides direct evidence that NLRP3 signaling is over-activated in IBD patients. The inhibition of NLRP3 reverses the IBD-like symptoms in DSS-induced mice, which the regulatory effects on gut microbiota might mediate. Overall, this present study provides a basis for the clinical application of NLRP3 as a target for IBD treatment.

Human study

The human body study was approved by the ethics review committee of the First Affiliated Hospital of Xiamen University (No.2022−038) and carried out in accordance with the Helsinki Declaration of the World Medical Association.

Animal study

All procedures are carried out in accordance with the guidelines of the Laboratory Animal Management Regulations and the Laboratory Animal Management System of Huaqiao University and have been approved by the Laboratory Animal Management Committee of Huaqiao University (A2021002).

Conflicts of interest

The authors declare that they have no conflicts of interest.

Acknowledgments

REFERENCES

[1] Perera AP, Fernando R, Shinde T, Gundamaraju R, Southam B, Sohal SS, et al. MCC950, a specific small molecule inhibitor of NLRP3 inflammasome attenuates colonic inflammation in spontaneous colitis mice. Sci Rep 2018;8(1):8618.

[2] Lee SH, Kwon JE, Cho ML. Immunological pathogenesis of inflammatory bowel disease. Intest Res 2018;16(1):26–42.

[3] Ng SC, Shi HY, Hamidi N, Underwood FE, Tang W, Benchimol EI, et al. Worldwide incidence and prevalence of inflammatory bowel disease in the 21st century: a systematic review of population-based studies. Lancet 2017;390(10114):2769–78.

[4] Kaplan GG. The global burden of IBD: from 2015 to 2025. Nat Rev Gastroenterol Hepatol 2015;12(12):720–7.

[5] Parray FQ, Wani ML, Malik AA, Wani SN, Bijli AH, Irshad I, et al. Ulcerative colitis: a challenge to surgeons. Int J Prev Med 2012;3(11):749–63.

[6] Guan Q. A comprehensive review and update on the pathogenesis of inflammatory bowel disease. J Immunol Res 2019;2019:7247238.

[7] Mentella MC, Scaldaferri F, Pizzoferrato M, Gasbarrini A, Miggiano GAD. Nutrition, IBD and gut microbiota: a review. Nutrients 2020;12(4):944.

[8] Zahid A, Li B, Kombe AJK, Jin T, Tao J. Pharmacological inhibitors of the NLRP3 inflammasome. Front Immunol 2019;10:2538.

[9] Li C, Qiu J, Xue Y. Low-dose Diosbulbin-B (DB) activates tumor-intrinsic PD-L1/NLRP3 signaling pathway mediated pyroptotic cell death to increase cisplatin-sensitivity in gastric cancer (GC). Cell Biosci 2021;11(1):38.

[10] Arango Duque G, Descoteaux A. Macrophage cytokines: involvement in immunity and infectious diseases. Front Immunol 2014;5:491.

[11] Zhang J, Liu X, Wan C, Liu Y, Wang Y, Meng C, et al. NLRP3 inflammasome mediates M1 macrophage polarization and IL-1β production in inflammatory root resorption. J Clin Periodontol 2020;47(4):451–60.

[12] Meng X, Zhang G, Cao H, Yu D, Fang X, de Vos WM, et al. Gut dysbacteriosis and intestinal disease: mechanism and treatment. J Appl Microbiol 2020;129(4):787–805.

[13] Zhang MM, Guo MX, Zhang QP, Chen XQ, Li NZ, Liu Q, et al. IL-1R/C3aR signaling regulates synaptic pruning in the prefrontal cortex of depression. Cell Biosci 2022;12(1):90.

[14] Nishida A, Inoue R, Inatomi O, Bamba S, Naito Y, Andoh A. Gut microbiota in the pathogenesis of inflammatory bowel disease. Clin J Gastroenterol 2018;11(1):1–10.

[15] Qiu P, Ishimoto T, Fu L, Zhang J, Zhang Z, Liu Y. The gut microbiota in inflammatory bowel disease. Front Cell Infect Microbiol 2022;12:733992.

[16] Kechagia M, Basoulis D, Konstantopoulou S, Dimitriadi D, Gyftopoulou K, Skarmoutsou N, et al. Health benefits of probiotics: a review. ISRN Nutr 2013;2013:481651.

[17] Yoon MY, Yoon SS. Disruption of the gut ecosystem by antibiotics. Yonsei Med J 2018;59(1):4–12.

[18] Weingarden AR, Vaughn BP. Intestinal microbiota, fecal microbiota transplantation, and inflammatory bowel disease. Gut Microb 2017;8(3):238–52.

[19] Hakansson A, Molin G. Gut microbiota and inflammation. Nutrients 2011;3(6):637–82.

[20] Zhang W, Zou G, Li B, Du X, Sun Z, Sun Y, et al. Fecal microbiota transplantation (FMT) alleviates experimental colitis in mice by gut microbiota regulation. J Microbiol Biotechnol 2020;30(8):1132–41.

[21] Fusco R, Siracusa R, Genovese T, Cuzzocrea S, Di Paola R. Focus on the role of NLRP3 inflammasome in diseases. Int J Mol Sci 2020;21(12):4223.

[22] Zaki MH, Boyd KL, Vogel P, Kastan MB, Lamkanfi M, Kanneganti TD. The NLRP3 inflammasome protects against loss of epithelial integrity and mortality during experimental colitis. Immunity 2010;32(3):379–91.

[23] Lazaridis LD, Pistiki A, Giamarellos-Bourboulis EJ, Georgitsi M, Damoraki G, Polymeros D, et al. Activation of NLRP3 inflammasome in inflammatory bowel disease: differences between Crohn's disease and ulcerative colitis. Dig Dis Sci 2017;62(9):2348–56.

[24] Kiesler P, Fuss IJ, Strober W. Experimental models of inflammatory bowel diseases. Cell Mol Gastroenterol Hepatol 2015;1(2):154–70.

[25] Randhawa PK, Singh K, Singh N, Jaggi AS. A review on chemical-induced inflammatory bowel disease models in rodents. KOREAN J PHYSIOL PHARMACOL 2014;18(4):279–88.

[26] Eichele DD, Kharbanda KK. Dextran sodium sulfate colitis murine model: an indispensable tool for advancing our understanding of inflammatory bowel diseases pathogenesis. World J Gastroenterol 2017;23(33):6016–29.

[27] Umiker B, Lee HH, Cope J, Ajami NJ, Laine JP, Fregeau C, et al. The NLRP3 inflammasome mediates DSS-induced intestinal inflammation in Nod2 knockout mice. Innate Immun 2019;25(2):132–43.

[28] Zhang YZ, Li YY. Inflammatory bowel disease: pathogenesis. World J Gastroenterol 2014;20(1):91–9.

[29] Gao X, Cao Q, Cheng Y, Zhao D, Wang Z, Yang H, et al. Chronic stress promotes colitis by disturbing the gut microbiota and triggering immune system response. Proc Natl Acad Sci U S A 2018;115(13):E2960–9.

[30] Kishida K, Kohyama M, Kurashima Y, Kogure Y, Wang J, Hirayasu K, et al. Negative regulation of DSS-induced experimental colitis by PILRα. Int Immunol 2015;27(6):307–14.

[31] Liu J, Zhang H, Su Y, Zhang B. Application and prospect of targeting innate immune sensors in the treatment of autoimmune diseases. Cell Biosci 2022;12(1):68.

[32] Mitra S, Sarkar A. Microparticulate P2X7 and GSDM-D mediated regulation of functional IL-1β release. Purinergic Signal 2019;15(1):119–23.

[33] Bulek K, Zhao J, Liao Y, Rana N, Corridoni D, Antanaviciute A, et al. Epithelial-derived gasdermin D mediates nonlytic IL-1β release during experimental colitis. J Clin Invest 2020;130(8):4218–34.

[34] Shao M, Yan Y, Zhu F, Yang X, Qi Q, Yang F, et al. Artemisinin analog SM934 alleviates epithelial barrier dysfunction via inhibiting apoptosis and caspase-1-mediated pyroptosis in experimental colitis. Front Pharmacol 2022;13:849014.

[35] Zhang S, Liang Y, Yao J, Li DF, Wang LS. Role of pyroptosis in inflammatory bowel disease (IBD): from gasdermins to DAMPs. Front Pharmacol 2022;13:833588.

[36] He Y, Zeng MY, Yang D, Metro B, Núñez G. NEK7 is an essential mediator of NLRP3 activation downstream of potassium efflux. Nature 2016;530(7590):354–7.

[37] Chen X, Liu G, Yuan Y, Wu G, Wang S, Yuan L. NEK7 interacts with NLRP3 to modulate the pyroptosis in inflammatory bowel disease via NF-κB signaling. Cell Death Dis 2019;10(12):906.

[38] Davis EM, Zhang D, Glover SC, Stappenbeck T, Wang SZ, Liu JJ. Inhibition of intestinal epithelial cell pyroptosis and associated mucosal barrier defects is a potential therapeutic mechanism of action for mesalamine in IBD. Gastroenterology 2019;156:S88.

[39] Coqueiro AY, Raizel R, Bonvini A, Tirapegui J, Rogero MM. Probiotics for inflammatory bowel diseases: a promising adjuvant treatment. Int J Food Sci Nutr 2019;70(1):20–9.

[40] Mishra K, Bukavina L, Ghannoum M. Symbiosis and dysbiosis of the human mycobiome. Front Microbiol 2021;12:636131.

[41] Ezeji JC, Sarikonda DK, Hopperton A, Erkkila HL, Cohen DE, Martinez SP, et al. Parabacteroides distasonis: intriguing aerotolerant gut anaerobe with emerging antimicrobial resistance and pathogenic and probiotic roles in human health. Gut Microbes 2021;13(1):1922241.

[42] Manichanh C, Rigottier-Gois L, Bonnaud E, Gloux K, Pelletier E, Frangeul L, et al. Reduced diversity of faecal microbiota in Crohn's disease revealed by a metagenomic approach. Gut 2006;55(2):205–11.

[43] Gophna U, Sommerfeld K, Gophna S, Doolittle WF, Veldhuyzen van Zanten SJ. Differences between tissue-associated intestinal microfloras of patients with Crohn's disease and ulcerative colitis. J Clin Microbiol 2006;44(11):4136–41.

[44] Vester-Andersen MK, Mirsepasi-Lauridsen HC, Prosberg MV, Mortensen CO, Träger C, Skovsen K, et al. Increased abundance of proteobacteria in aggressive Crohn's disease seven years after diagnosis. Sci Rep 2019;9(1):13473.

[45] Kabeerdoss J, Jayakanthan P, Pugazhendhi S, Ramakrishna BS. Alterations of mucosal microbiota in the colon of patients with inflammatory bowel disease revealed by real time polymerase chain reaction amplification of 16S ribosomal ribonucleic acid. Indian J Med Res 2015;142(1):23–32.

[46] Magne F, Gotteland M, Gauthier L, Zazueta A, Pesoa S, Navarrete P, et al. The firmicutes/bacteroidetes ratio: a relevant marker of gut dysbiosis in obese patients? Nutrients 2020;12(5):1474.

[47] Xu L, Zhang C, He D, Jiang N, Bai Y, Xin Y. Rapamycin and MCC950 modified gut microbiota in experimental autoimmune encephalomyelitis mouse by brain gut axis. Life Sci 2020;253:117747.